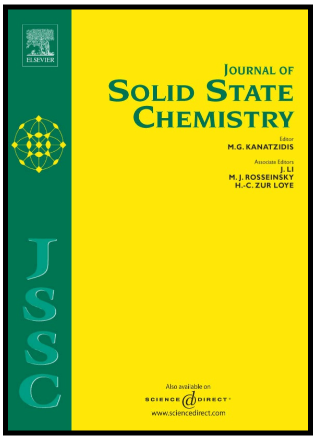

www.elsevier.com/locate/yjssc

A Luminescent Metal-Organic Framework with Pre-Designed Functionalized Ligands as an Efficient Fluorescence Sensing for Fe^{3+} Ions

Yeganeh Davoudabadi Farahani, Vahid Safarifard

PII: S0022-4596(18)30546-2
DOI: https://doi.org/10.1016/j.jssc.2018.12.005
Reference: YJSSC20506

To appear in: *Journal of Solid State Chemistry*

Received date: 24 October 2018
Revised date: 1 December 2018
Accepted date: 4 December 2018

Cite this article as: Yeganeh Davoudabadi Farahani and Vahid Safarifard, A Luminescent Metal-Organic Framework with Pre-Designed Functionalized Ligands as an Efficient Fluorescence Sensing for Fe^{3+} Ions, *Journal of Solid State Chemistry,* https://doi.org/10.1016/j.jssc.2018.12.005

A Luminescent Metal-Organic Framework with Pre-Designed Functionalized Ligands as an Efficient Fluorescence Sensing for Fe^{3+} Ions

Yeganeh Davoudabadi Farahani, Vahid Safarifard*[1]

Department of Chemistry, Iran University of Science and Technology, Tehran 16846-13114, Iran.

Email: vsafarifard@iust.ac.ir

Abstract:

Metal-organic frameworks are a class of attractive materials for fluorescent sensing. Here, we report the exploration of fluorescent Zn-based amine/azine-functionalized MOF, TMU-17-NH_2, ([Zn(NH_2-BDC)(4-bpdb)].2DMF; NH_2-BDC = amino-1,4-benzenedicarboxylic acid, 4-bpdb = 1,4-bis(4-pyridyl)-2,3-diaza-2,3-butadiene) for highly selective and sensitive detection of Fe^{3+} in DMF solution. TMU-17-NH_2 shows fast recognition of Fe^{3+} ion with a response time of <1 min and detection limit of 0.7 μM (40 ppb), and the luminescence is completely quenched in 10^{-3} M DMF solution of Fe^{3+}. Furthermore, the static quenching constant is calculated to be upper than 41000 M^{-1} by the fluorescence titration experiment in low concentration of Fe^{3+}. No interferences from 250 μM As^{3+}, Cd^{2+}, Zn^{2+}, Co^{3+}, Ni^{2+}, Cu^{2+}, Pb^{2+}, Mn^{2+} and Al^{3+} were found for the detection of Fe^{3+}. The efficient fluorescent quenching effect is attributed to the photoinduced electron transfer between Fe^{3+} ions and the amino-functionalized ligand in this MOF. Moreover, the introduced azine N donors in the 4-bpdb ligand of TMU-17-NH_2 additionally donate their lone-pair electrons to the Fe^{3+} ions, leading to significantly enhanced detection ability. Furthermore, the regenerated TMU-17-NH_2 still has high selectivity for Fe^{3+} ions, which suggests that the functionalized TMU-17-NH_2 is a promising luminescent probe for selectively sensing of Fe^{3+} ions.

Graphical abstract

Fluorescent Zn-based amine/azine-functionalized TMU-17-NH_2 MOF for highly selective and sensitive detection of Fe^{3+}.

---

[1] Tel: +98 21 77240540, Fax: +98 21 73021415

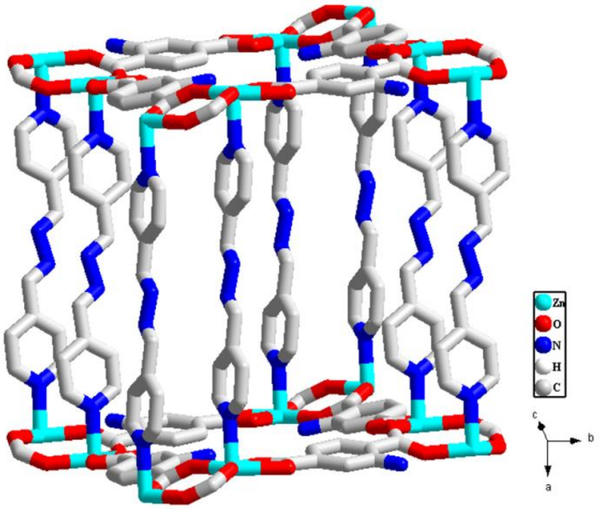

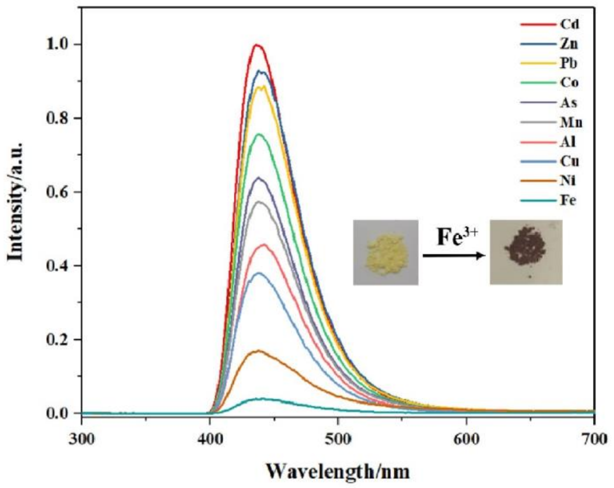

Keywords: Metal-Organic Frameworks; Fluorescence; Functionalization; Sensing; Fe^{3+}

1. Introduction

Metal ions play key roles in life and environment, and the detection of these metal ions is quite important. Iron is an important metal in industry [1]. However, its cationic form, Fe^{3+}, have different influences on the human body and other biological tissues. Fe^{3+} ion is one of the most essential elements for either humans or other living organisms on account of their significance in many biochemical processes and biological systems. Iron deficiency or excess both will lead to various severe function condition disorders, such as sleep loss, skin diseases, iron deficiency anemia and decreased immunity [2]. In addition, Fe^{3+} is a common inorganic pollutant in water. The presence of excess Fe^{3+} in drinking water could result in a number of problems related to human health. The recommended guideline level of Fe^{3+} in water is 0.3 ppm [3]. Therefore, the selective detection of Fe^{3+} is a very important subject in biological research as well as water treatment industry.

Various analytical techniques such as spectrophotometry, voltammetry and atomic absorption spectroscopy have been developed for determination of iron [4]. However, these analytical methods are often restricted by complicated sample preparation, sophisticated instruments and high cost. Therefore, it is important to develop efficient and economical approaches to sense and distinguish Fe^{3+} ions. Recently, fluorescent sensors have been considered as some of the promising and compelling devices for sensing metal ions or other small molecules because of their high sensitivity, good reliability, and real-time detection [5].

Metal-organic frameworks (MOFs), formed by the connection of metal centers or clusters and organic linkers through coordination bonding, have gathered immense attention due to not only their intriguing structures of diverse pore topologies and accessible cages and tunnels, unusual properties of permanent nanoscale porosity, high surface area, and the availability of in-pore functionality and outer-surface modification, but also their application potential in gas storage, separation, catalysis, proton conduction, sensing and so on [6-9]. In recent years, luminescent sensing with MOF materials has been considered as one of the most promising technologies for chemical and biological detection applications due to their easily induced luminescence, diverse advantages in structural and functional components, and various detecting mechanisms [10-12]. So far, an increasing number of luminescence MOFs have been reported and they have shown great potential as effective luminescence sensors important targets such as cations, anions, small molecules, gas, and vapors [13]. By the incorporation of guest molecules and ions into their pores, MOF fluorescence sensors can respond with different degrees of fluorescence enhancement or quenching behaviors [14].

Till now, several MOFs have shown good performance for the detection of Fe^{3+} ions [15-22]. However, the detection processes of these MOFs towards Fe^{3+} ions take relative long time because of the detection mechanisms of them are based on the ion exchange between the framework metal ions and Fe^{3+} ions [23-27]. Thus, there is an urgent need to develop new fluorescent MOF sensors for the selective and fast detection of Fe^{3+} ion [28, 29]. Amine and azine groups in organic luminescent materials are an electron-donating groups [30, 31], while metal ions often need to accept electrons. Therefore, these two functional groups in a luminescent MOF may be used as binding sites to bind with metal ions [32]. Encouraged by the above aspects, the work reported herein demonstrates that the highly luminescent MOF, $[Zn(NH_2\text{-}BDC)(4\text{-}bpdb)].2DMF$, (TMU-17-$NH_2$) reveals excellent potential for sensing Fe^{3+} ions. Mixed-linker microporous TMU-17-NH_2 consists of both amino-1,4-benzenedicarboxylic acid (NH_2-BDC) and the *N*,*N′*-bipyridine-type rigid linkers (4-bpdb = 1,4-bis(4-pyridyl)-2,3-diaza-2,3-butadiene) with ZnN_2O_4 secondary-building units (SBUs). TMU-17-NH_2 has been previously synthesized and reported for the selective synthesis of tetrahydro-chromenes, which the amine group of NH_2-BDC ligand has been found to be a base catalyst active site [33].

Very recently, a lot of studies on luminescent MOFs for sensing heavy metal ions such as Fe^{3+} and Cu^{2+} ions have been developed on the basis of interactions between metal ions and Lewis base sites within the ligands and energy or electron transfer from the ligand to metal ions [34-36]. Although excellent studies on a highly selective fluorescent probe for the detection of Fe^{3+} were reported by Zhou’s group [37], Sun’s group [20], and Wang’s group [38], the advantage of TMU-17-NH_2 is that the overall quenching constant for Fe^{3+} in the concentration range of 50-250 µM is quantified to be ~41000 M^{-1} and detection limit of 0.7 µM, which is comparable to that of other reports (Table 1). It is very exciting that TMU-17-NH_2, as a Fe^{3+}-probe, was not influenced by the presence of other metal ions such as As^{3+}, Cd^{2+}, Zn^{2+}, Co^{3+}, Ni^{2+}, Cu^{2+}, Pb^{2+}, Mn^{2+} and Al^{3+}. More importantly, the MOF could achieve recognition of Fe^{3+} ion in DMF solution with a response time of <1 min and 94% fluorescence quenching efficiency.

EXPERIMENTAL SECTION

Chemicals, Reagents and Apparatus.

Starting reagents for the synthesis were purchased and used without further purification from commercial suppliers (Sigma-Aldrich, Merck and others). $Zn(NO_3)_3·6H_2O$ and amino-1,4-benzenedicarboxylic acid (NH_2-BDC) were used to synthesize TMU-17-NH_2. N,N-Dimethylformamide (DMF) was used as the solvent to purify TMU-17-NH_2. Aqueous solutions of Cd^{2+}, Zn^{2+}, Pb^{2+}, Co^{2+}, As^{3+}, Mn^{2+}, Al^{3+}, Cu^{2+}, Ni^{2+} and Fe^{3+} were prepared from $CdCl_2·2.5H_2O$, $Zn(NO_3)_3·6H_2O$, $Pb(NO_3)_2$, $Co(NO_3)_2·6H_2O$, $NaAsO_2$, $Mn(OAc)_2·4H_2O$, $Al(NO_3)_3·9H_2O$, $Cu(NO_3)_2·3H_2O$, $NiCl_2·6H_2O$, and $Fe(NO_3)_3·9H_2O$, respectively. The infrared spectra were recorded on a Nicolet Fourier Transform IR, Nicolet 100 spectrometer in the range 500-4000 cm^{-1} using the KBr disk technique. X-ray powder diffraction (XRD) measurements were performed using a Philips X'pert diffractometer with monochromated Cu-k_α radiation (λ=1.54056Å). The simulated XRD powder pattern based on single crystal data was prepared using Mercury software [39]. The fluorescence experiments were performed at room temperature on a Shimadzu RF-6000 fluorescence spectrometer (kyoto, Japan) with a photomultiplier voltage of 700 V, scan speed of 60,000 nm min^{-1}, excitation slit width of 900 nm, emission slit width of 200-800 nm, and a 380 nm optical filter. The fluorescent emission spectra were recorded in the wavelength range of 300-800 nm upon excitation at 270 nm.

Preparation of 1,4-bis(4-pyridyl)-2,3-diaza-2,3-butadiene (4-bpdb).

1 mL (11 mmol) of hydrazine was added dropwise to a solution of pyridine-4-carboxaldehyde (2.2 mL, 22 mmol) dissolved in ethanol (15 mL). Two drops of formic acid were added and the mixture was stirred at room temperature for 24 h. The yellow solid that formed was filtered and washed several times with ethanol/ether (1:1). Yield, 79%.

Preparation of [Zn(NH_2-BDC)(4-bpdb)].2DMF (TMU-17-NH_2).

The TMU-17-NH_2, [Zn(NH_2-BDC)(4-bpdb)].2DMF was prepared by following the published protocol [33]. Briefly, $Zn(NO_3)_2·6H_2O$ (0.297 g, 1 mmol), 4-bpdb (0.210 g, 1 mmol), NH_2-BDC (0.181 g, 1 mmol) were dissolved in 15 ml DMF. The mixture was placed in a Teflon reactor and heated at 80 °C for 3 days, and then it was gradually cooled to room temperature during 24h. The crystals were obtained in a 33% yield. FT-IR (cm^{-1}): 3462.05 (s), 3364.90 (s), 1676.84 (vs), 1609.95 (vs), 1574.38 (vs), 1425.94 (vs), 1380.69 (vs), 1253.26 (s), 1094.03 (m), 1014.26 (m), 830.72 (s), 772.04 (s), 688.79 (s), 519.39 (s). Before luminescence process, the crystals were washed with 3 × 5 mL of DMF followed by 3 × 5 mL of CH_2Cl_2. The crystals were then soaked in 5 mL of CH_2Cl_2 for 3 days with fresh CH_2Cl_2 added every 24 h. After 3 days the CH_2Cl_2 solution was decanted, and the crystals were dried at 80 °C under vacuum for at least 24 h.

Luminescent Experiments.

TMU-17-NH_2 suspensions for fluorescence experiments were prepared by dispersing 1 mg of TMU-17-NH_2 powder in 4 mL of DMF under ultrasonication (80 W) for 10 min. To a 1 cm × 1 cm quartz cell, a TMU-17-NH_2 suspension (250 mg L^{-1}, 4 mL) and certain amounts (20 μL) of Fe^{3+} solution were sequentially added. The mixtures were then used for fluorescence measurements. The fluorescence data were collected after 5 min.

RESULTS AND DISCUSSION

Characterization of TMU-17-NH_2.

The MOF TMU-17-NH_2 has been previously synthesized and reported in the literature [33]. A guest-filled phase of TMU-17-NH_2, was synthesized by the solvothermal reaction of NH_2-BDC, 4-bpdb, and $Zn(NO_3)_2{\cdot}6H_2O$ in DMF at 80 °C for 72 h (Fig. 1a). TMU-17-NH_2 is a two-fold interpenetrated 3D framework bridged by dicarboxylates and 4-bpdb linkers. The 2D Zn-dicarboxylate layers are extended along the a-axis to form distorted square grids which are further pillared by 4-bpdb linkers along the b axis to form a 3D pillared-bilayer interpenetrated framework with a topology that can be described as a primitive cubic lattice (pcu) (Fig. 1b). As a results, the pore surface of TMU-17-NH_2 is decorated with pendant amine (-NH_2) and azine (=N-N=) functional groups. TMU-17-NH_2 has 1D channels of approximately 3 Å in cross section (including van der Waals radii) that are not large enough to be accessible for N_2 (kinetic diameters for N_2: 3.75 Å) adsorption. The experimental XRD pattern of the synthesized TMU-17-NH_2 was in good agreement with the simulated one [33], showing the successful preparation of TMU-17-NH_2 (Fig. 1c). To evaluate the thermal stability for further utilization, thermogravimetric analysis (TGA) of TMU-17-NH_2 was carried out under flowing N_2 atmosphere with the temperature range from 30 to 600 ℃ (Fig. 2a). The TG curve of the TMU-17-NH_2 presents two events. The first one is the elimination of the trapped solvents in the pores over the temperature range of ∼25-270 to form the guest-free phases, [Zn(NH_2-BDC)(4-bpdb)]. TMU-17-NH_2 material is thermally stable up to 300 ℃, above which the total decomposition of the organic ligand occurs, implying the good thermal stability of this MOF. The chemical stability of TMU-17-NH_2 was examined by suspending samples of the MOF in ethanol, acetonitrile, methanol, tetrahydrofuran, water and dichloromethane (Fig. 2b). TMU-17-NH_2 samples were immersed in the desired solvent overnight at ambient temperature. The MOF was found to be soluble in water, however, at the same time the PXRD patterns reveal that TMU-17-NH_2 can be resistant to the other solvents molecules.

Fluorescent Properties of TMU-17-NH_2.

The most significant structural feature of TMU-17-NH_2 is the presence of free amine and azine sites within the pores, highlighting the potential for its recognition of metal ions and thus for sensing functions. When TMU-17-NH_2 was dispersed in DMF solution, it has an emission peak at 440 nm with a weak luminescent intensity, as shown in Fig. 3a, which is approximately four times lower than the ligand NH_2-BDC dispersed in DMF. This interesting phenomenon can be attributed to the ligand-to-metal charge transfer (LMCT) effect upon the ligand NH_2-BDC coordination with Zn-O clusters to form the TMU-17-NH_2 framework. Furthermore, the solvent induced luminescence quenching effect may also play an important role in weakening the luminescent intensity of TMU-17-NH_2 in DMF solution, which was mainly dependent on the polarity of solvent molecules and their coupling with the Zn-O nodes as reported [40].

First of all, the luminescence properties of TMU-17-NH_2 in different solvent emulsions were investigated. Compound TMU-17-NH_2 (1 mg) was dispersed in different commonly used organic solvents (4 ml) like ethanol (EtOH), methanol (MeOH), N,N′-dimethylformamide (DMF), tetrahydrofuran (THF), dichloromethane (CH_2Cl_2) and acetonitrile (MeCN). As shown in Figure 3b, the PL intensity is largely dependent on the solvent molecules, particularly in the case of DMF, which exhibited the most significant enhancing effects. Shifts in emission are observed upon changing the solvent, and the wavelength corresponding to the maximum peak decreases in the order DMF > CH_3CN > CH_2Cl_2 > EtOH > THF > MeOH (Fig. 3c).

To examine the potential of TMU-17-NH_2 for sensing metal ions, the activated TMU-17-NH_2 (1 mg) was immersed in 4 mL DMF solutions containing $M(NO_3)_x$ (M = Zn^{2+}, Pb^{2+}, Co^{2+}, Cu^{2+}, Cd^{2+}, Al^{3+}, or Fe^{3+}), $NaAsO_2$, $Mn(OAc)_2$ and $NiCl_2$ to form the metal ion incorporated MOF suspension for luminescence studies. The suspension-state luminescent measurements illustrated that various metal ions display markedly different effects on the luminescence intensity of TMU-17-NH_2. As shown in Figure 4a-b, the luminescence intensity of TMU-17-NH_2 shows the quenching effect for all metal ions, but the quenching degree is heavily dependent on the species of metal ions. Among the metal ions studied, the quenching effects of Fe^{3+}, Ni^{2+} and Cu^{2+} are very pronounced, especially for Fe^{3+} ions. Moreover, the color changes seen by the naked eye have also been recorded (Fig. 4b, inset). After Fe^{3+} is incorporated, the luminescence intensity of the TMU-17-NH_2 suspension reduces to 0.04 from 1. The luminescence intensity of TMU-17-NH_2 (metal-ion free) was quenched by about 96, 83 and 62% when incorporated with Fe^{3+}, Ni^{2+} and Cu^{2+}, respectively. Obvious color change from bright yellow to brownish red of the TMU-17-NH_2 solid samples was also observed after the Fe^{3+} incorporation (Fig. 4a, inset). Clearly, TMU-17-NH_2 can highly efficiently sense Fe^{3+} ions through the fluorescent quenching, which can also be easily recognized by the naked-eye.

The chemically closely related metal ions can frequently interfere with ion binding. So, to examine the selective detection of TMU-17-NH_2 on Fe^{3+}, the quenching effects of Ni^{2+} and Cu^{2+} on the luminescence intensity of MOF must be considered. We studied the optical properties of the M^{n+}@TMU-17-NH_2 (M = Fe^{3+}, Ni^{2+} and Cu^{2+}) when immersing in different concentrations of metal cations (Fig. 5). It is obvious that the luminescence intensity at 440 nm is gradually decreased as the concentration of the metal cations increase. As demonstrated in Figure 4a, when the Fe^{3+} concentration increased from 0 to 1000 μM, the emission intensity of TMU-17-NH_2 was gradually decreased and a good linear relationship (correlation coefficient R = 0.997) between the emission intensity of TMU-17-NH_2 and the concentration of Fe^{3+} was observed in the range of 0-250 μM of Fe^{3+} (Fig. 5a; inset). The luminescence intensity of the Fe^{3+}-incorporated TMU-17-NH_2 from a 50 μM DMF solution of $Fe(NO_3)_3$ is about half that of the metal-ion free MOF, indicating the potential of TMU-17-NH_2 for the sensing of Fe^{3+}.

The fluorescence quenching follows the Stern-Völmer (SV) equation: $I_0/I=1 + K_{SV}[M]$, where I_0 and I correspond to the luminescence intensity for TMU-17-NH_2 in absence and presence of metal cations, respectively, [M] is the metal concentration, and K_{SV} is the Stern-Völmer constant. It is thus expected that the reduction in luminescence intensity is proportional to the concentration of the metal ion. It was found that the SV plot of TMU-17-NH_2 towards Fe^{3+} ions is nearly linear at low concentration range, but subsequently deviates from linearity and bends upwards at higher concentrations (Fig. 5a; inset). Moreover, the K_{SV} is calculated via luminescent data. An exceptionally high K_{SV} value of 41565 M^{-1} was obtained for Fe^{3+}, while K_{SV} for Ni^{2+} and Cu^{2+} were 16180 and 5766 M^{-1}, respectively. For metal ion-incorporated TMU-17-NH_2, $K_{SV}[Fe^{3+}]/K_{SV}[Ni^{2+}]$ and $K_{SV}[Fe^{3+}]/K_{SV}[Cu^{2+}]$ are 2.6 and 7.2, respectively, in which $K_{SV}[M^{n+}]$ represent the K_{SV} of M^{n+}@TMU-17-NH_2. Obviously, TMU-17-NH_2 shows highly selective sensing for Fe^{3+} ions (see Fig. 5d). The sensitivity of TMU-17-NH_2 is three to four orders of magnitude higher than that for previously reported MOFs with K_{SV} values in the range of tens to hundreds M^{-1} (Table 1). The high sensitivity allows us to easily identify the existence of a small amount of Fe^{3+} ions.

To further corroborate the high sensitivity of TMU-17-NH_2 compared to other reported systems, we determined the detection limit for Fe^{3+} on the basis of the 3δ IUPAC criterion [41, 42]. Based on the slope of the calibration curve (K) values and the standard deviations (S_b) from ten repeated fluorescent measurements of blank solutions, the detection limits ($3S_b/K$) of TMU-17-NH_2 towards Fe^{3+} ion in DMF were calculated to be 0.7 μM (corresponding to 40 ppb). This is also comparable to or better than some previously reported Fe^{3+} fluorescent sensors (Table 1)

Additionally, to investigate the time-response characteristic of the TMU-17-NH_2 sensor toward Fe^{3+}, the fluorescence intensity of TMU-17-NH_2 (λ_{ex} = 270 nm) was measured as a function of immersion time in DMF solution of 100 μM Fe^{3+} (Fig. 6a). With increasing time, the PL intensity decreases for the Fe^{3+}-loaded sample. Fe^{3+} induced fluorescence quenching reaction is very fast. The emission intensity of TMU-17-NH_2 at 440 nm has been decreased to more than 6.7 times in less than 1 min and a constant value in 8 min (Fig. 6a). This response is much faster than that in the some previous reports (about 24 h or 72 h). This rapid response is quite appealing and may be attribute to the fact that Fe^{3+} ions can rapidly diffuse into the channels of TMU-17-NH_2 and interact with luminophores on the pore surface.

It should be pointed out that usually many metal ions coexist in practical biological and environmental systems. Further experiments for the effect of coexisting metal ions on the quenched fluorescence intensity of TMU-17-NH_2 by Fe^{3+} were performed to show the selectivity of TMU-17-NH_2 for detecting Fe^{3+} (Fig. 6b). It is very encouraging that TMU-17-NH_2 shows high anti-interference from other coexisting metal ions. The tolerable concentrations of the interfering metal ion with the detection of 150 μM Fe^{3+} were 250 μM for Co^{2+}, Cu^{2+}, Mn^{2+}, Ni^{2+}, Cd^{2+}, Al^{3+} or As^{3+}. It is quite cheerful that the quenching effect of the Fe^{3+} ion on TMU-17-NH_2-luminescence is not influenced by the addition of other metal ions, further underlining the high selectivity of this MOF for detecting Fe^{3+} and the great potential of TMU-17-NH_2 for real sample application.

According to the above studies, we attempted to explore the possible sensing mechanism of fluorescence quenching for Fe^{3+}. Generally, the reasons for the fluorescence quenching caused by MOFs can be attributed to the following reasons: the ionic exchange, the collapse or change of the structure, and the competitive photon absorption between the adsorbed ions and MOFs [43]. The PXRD measurements were carried out to study the structures of the original and metal ion incorporated MOF samples of Fe^{3+}@TMU-17-NH_2. As shown in Fig. 2b, the PXRD patterns of the Fe^{3+}@TMU-17-NH_2 is similar to that of TMU-17-NH_2 ruling out the collapse of the MOF framework. We infer that the energy transfer may be responsible for the quenching phenomenon. According to the reported literature, porous MOFs with Lewis basic sites, such as pyridyl, amide, anionic sulfonate sites, can have significant interactions with guest metal ions [44, 45]. We therefore suggest that the quenching might be related to the interaction between the Fe^{3+} ions and pendant amine and azine functional groups in TMU-17-NH_2. The interaction between the Fe^{3+} ions and the NH_2-BDC ligands minimizes the energy transfer efficiency from NH_2-BDC to the Zn^{2+} ions within TMU-17-NH_2, thus decreasing the luminescence intensity.

As a sensor, regeneration is another important issue. The reusability of the fluorescence sensing performances of the MOF probe towards Fe^{3+} ions was examined up to four cycles. For checking its recyclability, the MOF compound was filtered off after each fluorescence titration experiment. The filtered materials were washed with DMF repeatedly and then dried in an oven. TMU-17-NH_2 showed outstanding recovery of its initial fluorescence intensity, even after four consecutive cycles of fluorescence sensing experiments, demonstrating its good recyclability and stability for the detection applications (Fig. 6c).

CONCLUSIONS

Lewis basic sites within porous MOFs are expected to play very important roles for their recognition of small Lewis acidic molecules and metal ions, and thus to find functionalities in chemical transformation and sensing. Here we used the amine-functionalized dicarboxylate ligand as well as the ligand contain a bridging azine group in the middle to functionalize the TMU-17-NH_2 luminescent MOF as a stable fluorescent sensor for detecting Fe^{3+}. This luminescent probe shows high selectivity for sensing Fe^{3+} in DMF solution with excellent sensitivity (K_{sv} ~ 41000 M^{-1}) and a detection limit of 0.7 μM, and fast response speed (<1 min). The present results may provide a facile route to design and synthesize functional MOFs with applications in fluorescent sensors.

ACKNOWLEDGMENTS

Support of this investigation by Iran University of Science and Technology and Iran's National Elites Foundation is gratefully acknowledged.

REFERENCES

[1] P. Nelson, Important elements, J. Chem. Educ., 68 (1991) 732.
[2] L.M. Hyman, K.J. Franz, Probing oxidative stress: Small molecule fluorescent sensors of metal ions, reactive oxygen species, and thiols, Coord. Chem. Rev., 256 (2012) 2333-2356.
[3] W.H. Organization, Guidelines for drinking-water quality: recommendations, World Health Organization, 2004.
[4] K. Akatsuka, J.W. McLaren, J.W. Lam, S.S. Berman, Determination of iron and ten other trace elements in the open ocean seawater reference material NASS-3 by inductively coupled plasma mass spectrometry, J. Anal. At. Spectrom., 7 (1992) 889-894.
[5] L.E. Kreno, K. Leong, O.K. Farha, M. Allendorf, R.P. Van Duyne, J.T. Hupp, Metal–organic framework materials as chemical sensors, Chem. Rev., 112 (2011) 1105-1125.
[6] M.I.H. Mohideen, R.S. Pillai, K. Adil, P.M. Bhatt, Y. Belmabkhout, A. Shkurenko, G. Maurin, M. Eddaoudi, A Fine-Tuned MOF for Gas and Vapor Separation: A Multipurpose Adsorbent for Acid Gas Removal, Dehydration, and BTX Sieving, Chem, 3 (2017) 822-833.
[7] R.W. Flaig, T.M. Osborn Popp, A.M. Fracaroli, E.A. Kapustin, M.J. Kalmutzki, R.M. Altamimi, F. Fathieh, J.A. Reimer, O.M. Yaghi, The Chemistry of CO_2 Capture in an Amine-Functionalized Metal–Organic Framework under Dry and Humid Conditions, J. Am. Chem. Soc., 139 (2017) 12125-12128.
[8] S. Kazemi, V. Safarifard, Carbon dioxide capture in MOFs: The effect of ligand functionalization, Polyhedron, 154 (2018) 236-251.
[9] M. Tanhaei, A.R. Mahjoub, V. Safarifard, Ultrasonic-assisted synthesis and characterization of nanocomposites from azine-decorated metal-organic framework and graphene oxide layers, Mater. Lett., 227 (2018) 318-321.
[10] Y. Su, J. Yu, Y. Li, S.F.Z. Phua, G. Liu, W.Q. Lim, X. Yang, R. Ganguly, C. Dang, C. Yang, Versatile bimetallic lanthanide metal-organic frameworks for tunable emission and efficient fluorescence sensing, Commun. Chem., 1 (2018) 12.
[11] Y. Zhang, S. Yuan, G. Day, X. Wang, X. Yang, H.-C. Zhou, Luminescent sensors based on metal-organic frameworks, Coord. Chem. Rev., 354 (2017) 28-45.
[12] Z. Hu, B.J. Deibert, J. Li, Luminescent metal–organic frameworks for chemical sensing and explosive detection, Chem. Soc. Rev., 43 (2014) 5815-5840.
[13] J.-N. Hao, B. Yan, A water-stable lanthanide-functionalized MOF as a highly selective and sensitive fluorescent probe for Cd^{2+}, Chem. Commun., 51 (2015) 7737-7740.
[14] Y.-W. Li, J.-R. Li, L.-F. Wang, B.-Y. Zhou, Q. Chen, X.-H. Bu, Microporous metal–organic frameworks with open metal sites as sorbents for selective gas adsorption and fluorescence sensors for metal ions, J. Mater. Chem. A, 1 (2013) 495-499.
[15] X.-H. Zhou, L. Li, H.-H. Li, A. Li, T. Yang, W. Huang, A flexible Eu(III)-based metal–organic framework: turn-off luminescent sensor for the detection of Fe(III) and picric acid, Dalton Trans., 42 (2013) 12403-12409.
[16] M.-L. Gao, N. Wei, Z.-B. Han, Anionic metal–organic framework for high-efficiency pollutant removal and selective sensing of Fe(III) ions, RSC Adv., 6 (2016) 60940-60944.

[17] Y.-F. Li, D. Wang, Z. Liao, Y. Kang, W.-H. Ding, X.-J. Zheng, L.-P. Jin, Luminescence tuning of the Dy–Zn metal–organic framework and its application in the detection of Fe(iii) ions, J. Mater. Chem. C, 4 (2016) 4211-4217.

[18] Z. Xiang, C. Fang, S. Leng, D. Cao, An amino group functionalized metal–organic framework as a luminescent probe for highly selective sensing of Fe^{3+} ions, J. Mater. Chem. A, 2 (2014) 7662-7665.

[19] X.-L. Zhao, D. Tian, Q. Gao, H.-W. Sun, J. Xu, X.-H. Bu, A chiral lanthanide metal–organic framework for selective sensing of Fe(III) ions, Dalton Trans., 45 (2016) 1040-1046.

[20] Z. Chen, Y. Sun, L. Zhang, D. Sun, F. Liu, Q. Meng, R. Wang, D. Sun, A tubular europium–organic framework exhibiting selective sensing of Fe^{3+} and Al^{3+} over mixed metal ions, Chem. Commun., 49 (2013) 11557-11559.

[21] Y. Kang, X.-J. Zheng, L.-P. Jin, A microscale multi-functional metal-organic framework as a fluorescence chemosensor for Fe(III), Al(III) and 2-hydroxy-1-naphthaldehyde, J. Colloid Interface Sci., 471 (2016) 1-6.

[22] Q. Tang, S. Liu, Y. Liu, J. Miao, S. Li, L. Zhang, Z. Shi, Z. Zheng, Cation sensing by a luminescent metal–organic framework with multiple Lewis basic sites, Inorg. Chem., 52 (2013) 2799-2801.

[23] C.-X. Yang, H.-B. Ren, X.-P. Yan, Fluorescent metal–organic framework MIL-53(Al) for highly selective and sensitive detection of Fe^{3+} in aqueous solution, Anal. Chem., 85 (2013) 7441-7446.

[24] M. Zheng, H. Tan, Z. Xie, L. Zhang, X. Jing, Z. Sun, Fast response and high sensitivity europium metal organic framework fluorescent probe with chelating terpyridine sites for Fe^{3+}, ACS Appl. Mater. Interfaces, 5 (2013) 1078-1083.

[25] R. Wang, X.-Y. Dong, H. Xu, R.-B. Pei, M.-L. Ma, S.-Q. Zang, H.-W. Hou, T.C. Mak, A super water-stable europium–organic framework: guests inducing low-humidity proton conduction and sensing of metal ions, Chem. Commun., 50 (2014) 9153-9156.

[26] L.H. Cao, F. Shi, W.M. Zhang, S.Q. Zang, T.C. Mak, Selective Sensing of Fe^{3+} and Al^{3+} Ions and Detection of 2, 4, 6- Trinitrophenol by a Water- Stable Terbium- Based Metal–Organic Framework, Chem. Eur. J., 21 (2015) 15705-15712.

[27] Y. Zhou, H.-H. Chen, B. Yan, An Eu^{3+} post-functionalized nanosized metal–organic framework for cation exchange-based Fe^{3+}-sensing in an aqueous environment, J. Mater. Chem. A, 2 (2014) 13691-13697.

[28] L. Li, Q. Chen, Z. Niu, X. Zhou, T. Yang, W. Huang, Lanthanide metal–organic frameworks assembled from a fluorene-based ligand: Selective sensing of Pb^{2+} and Fe^{3+} ions, J. Mater. Chem. C, 4 (2016) 1900-1905.

[29] S. Dang, E. Ma, Z.-M. Sun, H. Zhang, A layer-structured Eu-MOF as a highly selective fluorescent probe for Fe^{3+} detection through a cation-exchange approach, J. Mater. Chem., 22 (2012) 16920-16926.

[30] S. Maruyama, K. Kikuchi, T. Hirano, Y. Urano, T. Nagano, A novel, cell-permeable, fluorescent probe for ratiometric imaging of zinc ion, J. Am. Chem. Soc., 124 (2002) 10650-10651.

[31] X. Peng, J. Du, J. Fan, J. Wang, Y. Wu, J. Zhao, S. Sun, T. Xu, A selective fluorescent sensor for imaging Cd^{2+} in living cells, J. Am. Chem. Soc., 129 (2007) 1500-1501.

[32] Z. Xiang, C. Fang, S. Leng, D. Cao, An amino group functionalized metal-organic framework as a luminescent probe for highly selective sensing of Fe^{3+} ions, J. Mater. Chem. A, 2 (2014) 7662-7665.

[33] V. Safarifard, S. Beheshti, A. Morsali, An interpenetrating amine-functionalized metal-organic framework as an efficient and reusable catalyst for the selective synthesis of tetrahydro-chromenes, CrystEngComm, 17 (2015) 1680-1685.

[34] Z. Xiang, Z. Hu, D. Cao, W. Yang, J. Lu, B. Han, W. Wang, Metal–organic frameworks with incorporated carbon nanotubes: improving carbon dioxide and methane storage capacities by lithium doping, Angewandte Chemie International Edition, 50 (2011) 491-494.

[35] Z. Xiang, D. Cao, Porous covalent–organic materials: synthesis, clean energy application and design, J. Mater. Chem. A, 1 (2013) 2691-2718.

[36] Y.-S. Bae, K.L. Mulfort, H. Frost, P. Ryan, S. Punnathanam, L.J. Broadbelt, J.T. Hupp, R.Q. Snurr, Separation of CO_2 from CH_4 using mixed-ligand metal−organic frameworks, Langmuir, 24 (2008) 8592-8598.

[37] X. Zhou, H. Li, H. Xiao, L. Li, Q. Zhao, T. Yang, J. Zuo, W. Huang, A microporous luminescent europium metal–organic framework for nitro explosive sensing, Dalton Trans., 42 (2013) 5718-5723.

[38] X.-Y. Dong, R. Wang, J.-Z. Wang, S.-Q. Zang, T.C. Mak, Highly selective Fe^{3+} sensing and proton conduction in a water-stable sulfonate–carboxylate Tb–organic-framework, J. Mater. Chem. A, 3 (2015) 641-647.

[39] (Mercury 1.4.1, Copyright Cambridge Crystallographic Data Centre, 12 Union Road, Cambridge, CB2 1EZ, UK, 2001-2005).

[40] M. Wang, L. Guo, D. Cao, Metal-organic framework as luminescence turn-on sensor for selective detection of metal ions: Absorbance caused enhancement mechanism, Sens. Actuator B-Chems., 256 (2018) 839-845.

[41] G.L. Long, J.D. Winefordner, Limit of detection. A closer look at the IUPAC definition, Anal. Chem., 55 (1983) 712A-724A.

[42] S.A.A. Razavi, M.Y. Masoomi, A. Morsali, Double Solvent Sensing Method for Improving Sensitivity and Accuracy of Hg(II) Detection Based on Different Signal Transduction of a Tetrazine-Functionalized Pillared Metal–Organic Framework, Inorg. Chem., 56 (2017) 9646-9652.

[43] J. Hu, T. Cheng, S. Dong, C. Zhou, X. Huang, L. Zhang, Multifunctional luminescent Cd(II)-based metal-organic framework material for highly selective and sensitive sensing 2, 4, 6-trinitrophenol (TNP) and Fe^{3+} cation, Micropor. Mesopor. Mater., 272 (2018) 177-183.

[44] J.-R. Li, R.J. Kuppler, H.-C. Zhou, Selective gas adsorption and separation in metal–organic frameworks, Chem. Soc. Rev., 38 (2009) 1477-1504.

[45] B. Gole, A.K. Bar, P.S. Mukherjee, Fluorescent metal–organic framework for selective sensing of nitroaromatic explosives, Chem. Commun., 47 (2011) 12137-12139.

[46] B. Wang, Q. Yang, C. Guo, Y. Sun, L.-H. Xie, J.-R. Li, Stable Zr(IV)-based metal–organic frameworks with predesigned functionalized ligands for highly selective detection of Fe(III) ions in water, ACS Appl. Mater. Interfaces, 9 (2017) 10286-10295.

[47] S. Chen, Z. Shi, L. Qin, H. Jia, H. Zheng, Two New Luminescent Cd(II)-Metal–Organic Frameworks as Bifunctional Chemosensors for Detection of Cations Fe^{3+}, Anions CrO_4^{2-}, and $Cr_2O_7^{2-}$in Aqueous Solution, Cryst. Growth Des., 17 (2016) 67-72.

[48] B. Parmar, Y. Rachuri, K.K. Bisht, E. Suresh, Mixed-Ligand LMOF Fluorosensors for Detection of Cr(VI) Oxyanions and Fe^{3+}/Pd^{2+} Cations in Aqueous Media, Inorg. Chem., 56 (2017) 10939-10949.

[49] S.T. Zhang, J. Yang, H. Wu, Y.Y. Liu, J.F. Ma, Systematic Investigation of High- Sensitivity Luminescent Sensing for Polyoxometalates and Iron(III) by MOFs Assembled with a New Resorcin [4] arene- Functionalized Tetracarboxylate, Chem. Eur. J., 21 (2015) 15806-15819.

[50] W. Yan, C. Zhang, S. Chen, L. Han, H. Zheng, Two lanthanide metal–organic frameworks as remarkably selective and sensitive bifunctional luminescence sensor for metal ions and small organic molecules, ACS Appl. Mater. Interfaces, 9 (2017) 1629-1634.

[51] Y.-J. Yang, M.-J. Wang, K.-L. Zhang, A novel photoluminescent Cd(ii)–organic framework exhibiting rapid and efficient multi-responsive fluorescence sensing for trace amounts of Fe^{3+} ions and some NACs, especially for 4-nitroaniline and 2-methyl-4-nitroaniline, J. Mater. Chem. C, 4 (2016) 11404-11418.

[52] H. Zhang, R. Fan, W. Chen, J. Fan, Y. Dong, Y. Song, X. Du, P. Wang, Y. Yang, 3D lanthanide metal–organic frameworks based on mono-, tri-, and heterometallic tetranuclear clusters as highly selective and sensitive luminescent sensor for Fe^{3+} and Cu^{2+} ions, Cryst. Growth Des., 16 (2016) 5429-5440.

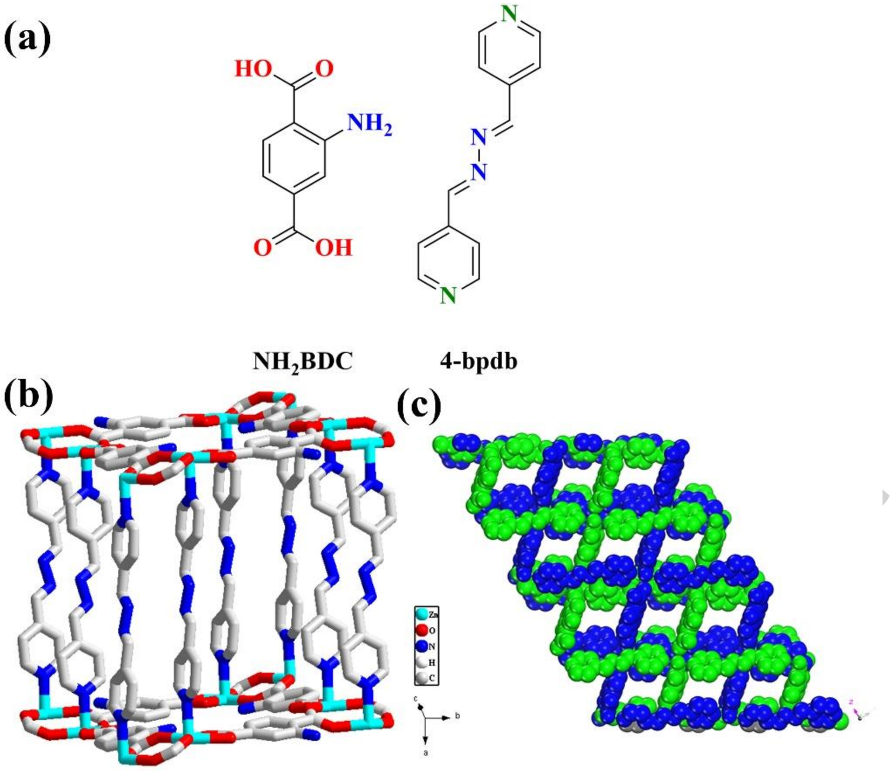

Figure 1. (a) Chemical Structure of NH_2-BDC and 4-bpdb. (b) Structure of the cuboidal block of TMU-17-NH_2, showing Zn units linked by eight NH_2-BDC and eight 4-bpdb units; (c) Representations of the structure of the open phase TMU-17-NH_2 which contains 1D channels. The two interpenetrating frameworks are shown in blue and green. The disordered guest molecules are omitted for clarity.

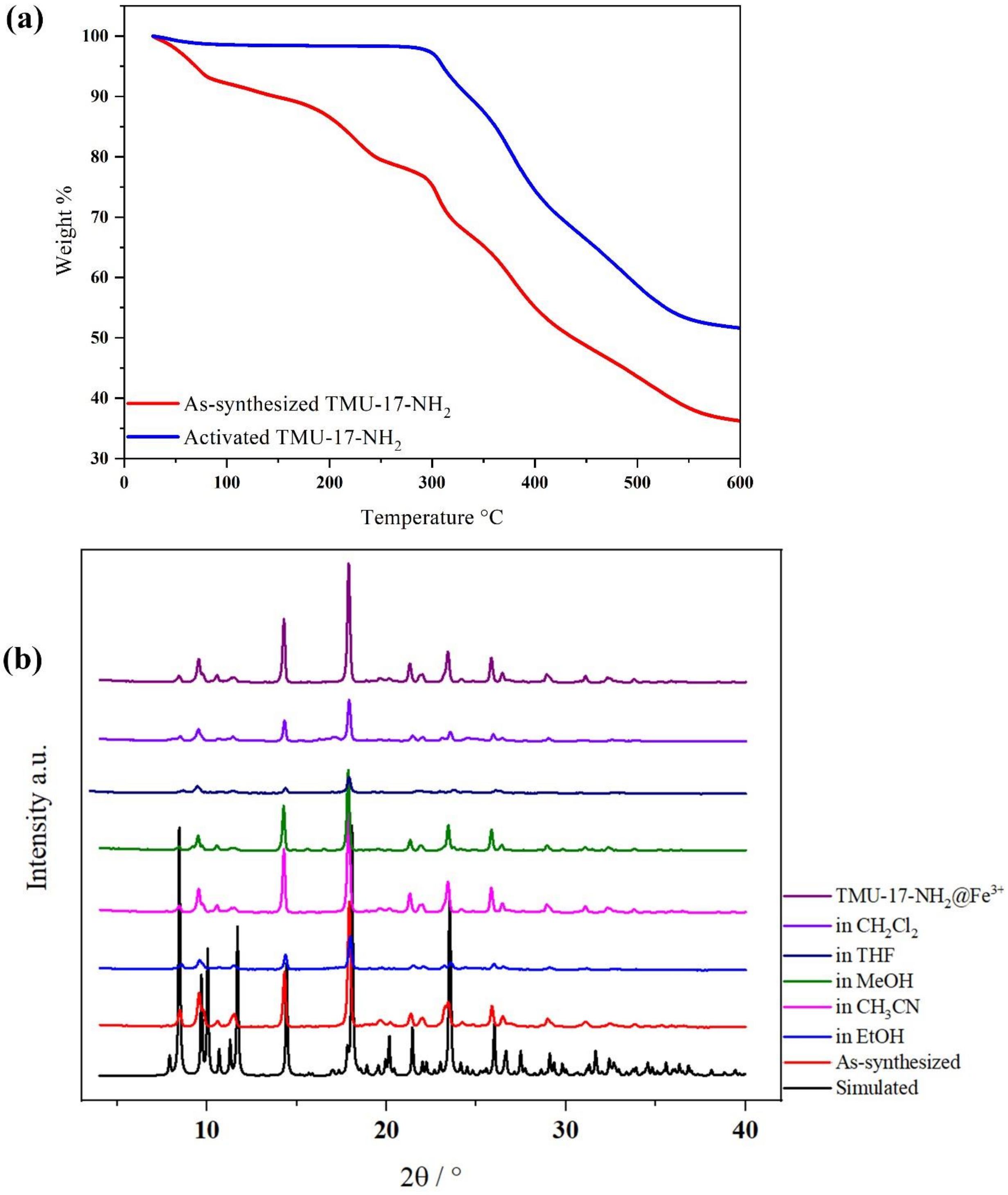

Figure 2. (a) TGA of as-synthesized (red) and activated TMU-17-NH$_2$ (blue). (b) PXRD of TMU-17-NH$_2$: as-synthesized (red), simulated (black); immersed in EtOH (blue), CH$_3$CN (pink), MeOH (green), THF (dark blue), CH$_2$Cl$_2$ (purple) and TMU-17-NH$_2$@Fe^{3+} (dark purple).

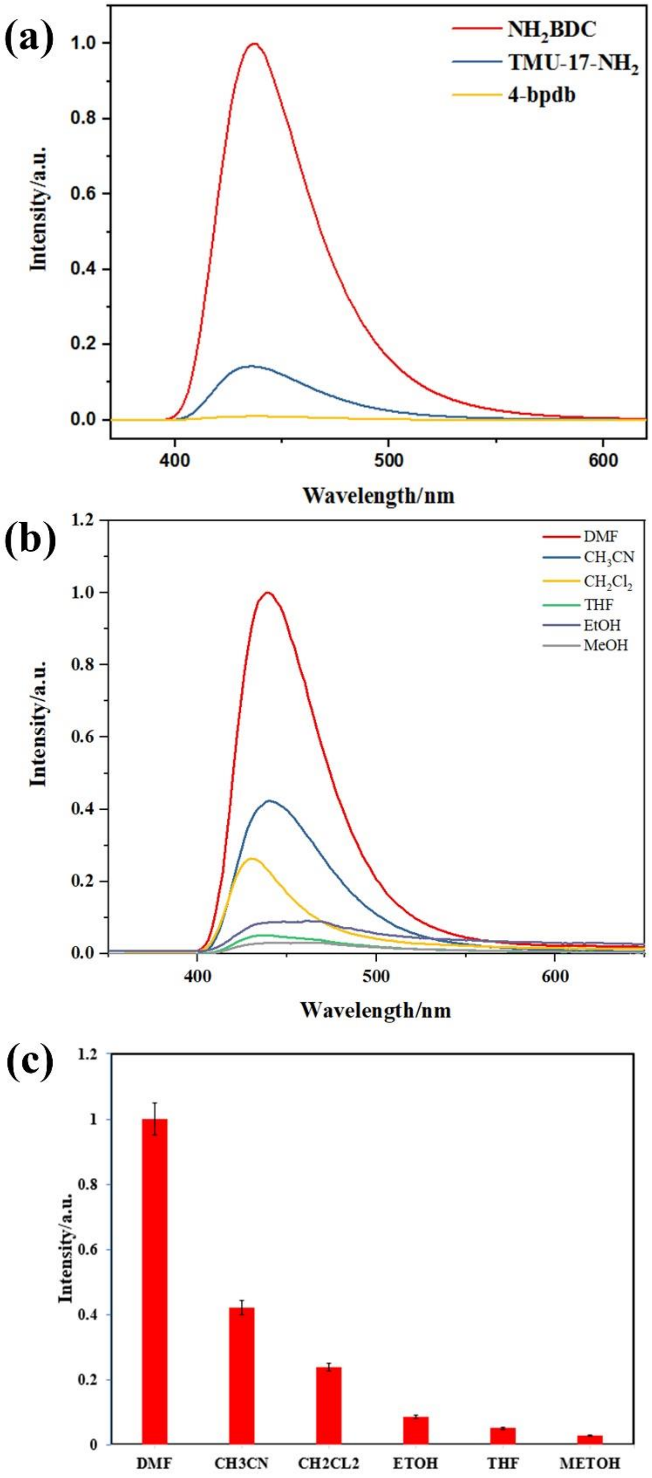

Figure 3. (a) The PL spectra of TMU-17-NH_2 (blue), NH_2-BDC (red) and 4-bpdb (yellow) suspensions in DMF. (b) The PL spectra of TMU-17-NH_2-solvent emulsions at room temperature, where the red, blue, yellow, purple, green and gray curves denote the intensities of TMU-17-NH_2-DMF, -CH_3CN, -CH_2Cl_2, -EtOH, -THF and -MeOH, respectively. (c) Comparisons of the luminescence intensity of TMU-17-NH_2-solvent emulsions at room temperature.

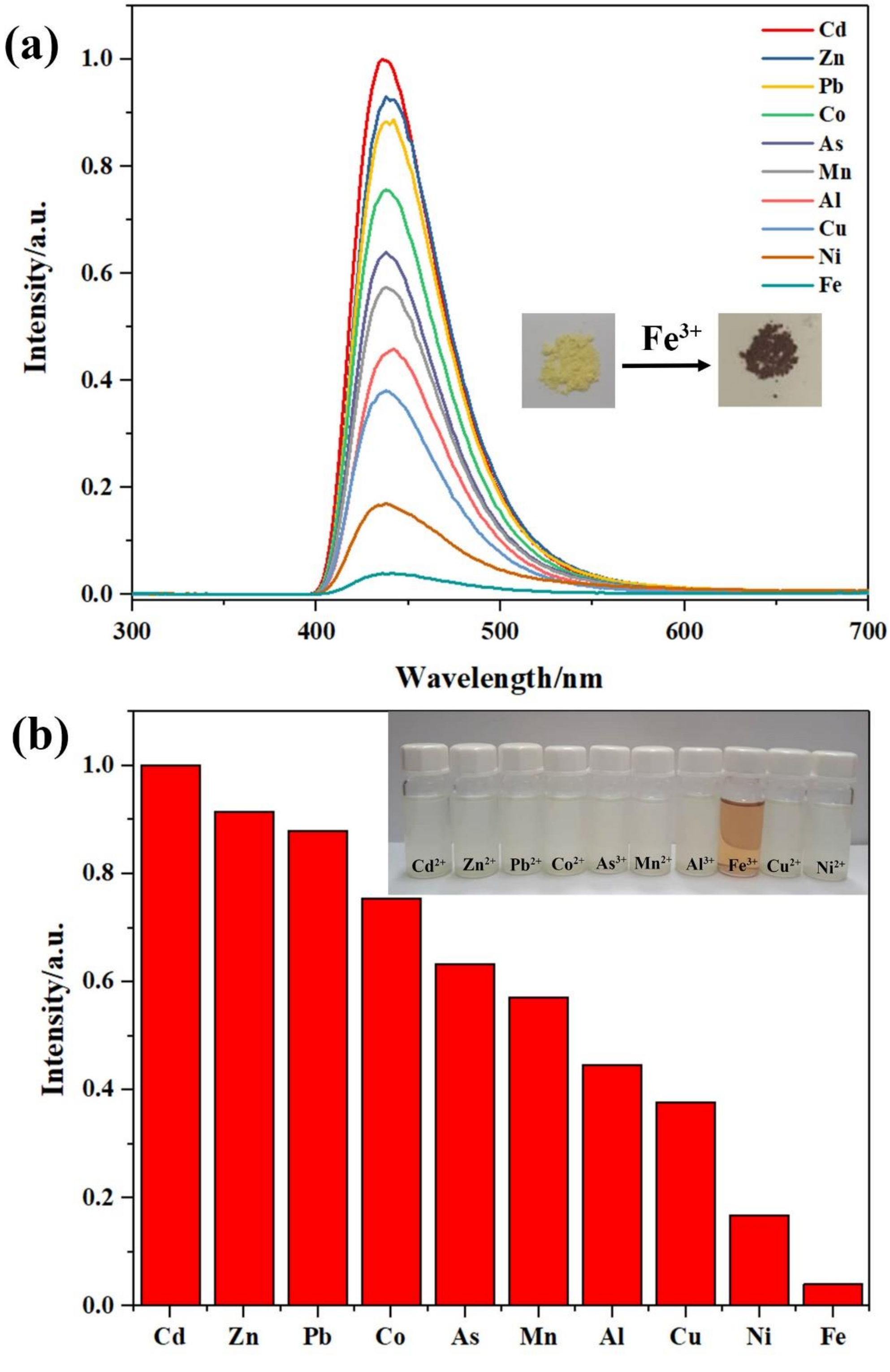

Figure 4. (a) Emission spectra of TMU-17-NH_2 (1 mg) in DMF (4 ml) with various metal ions (250 μM). (Inset: photographs of Fe^{3+}@TMU-17-NH_2 sample as solid). (b) Relative luminescence intensities of M^{n+}@TMU-17-NH_2 in DMF. (Inset: photographs of M^{n+}@TMU-17-NH_2 sample in DMF).

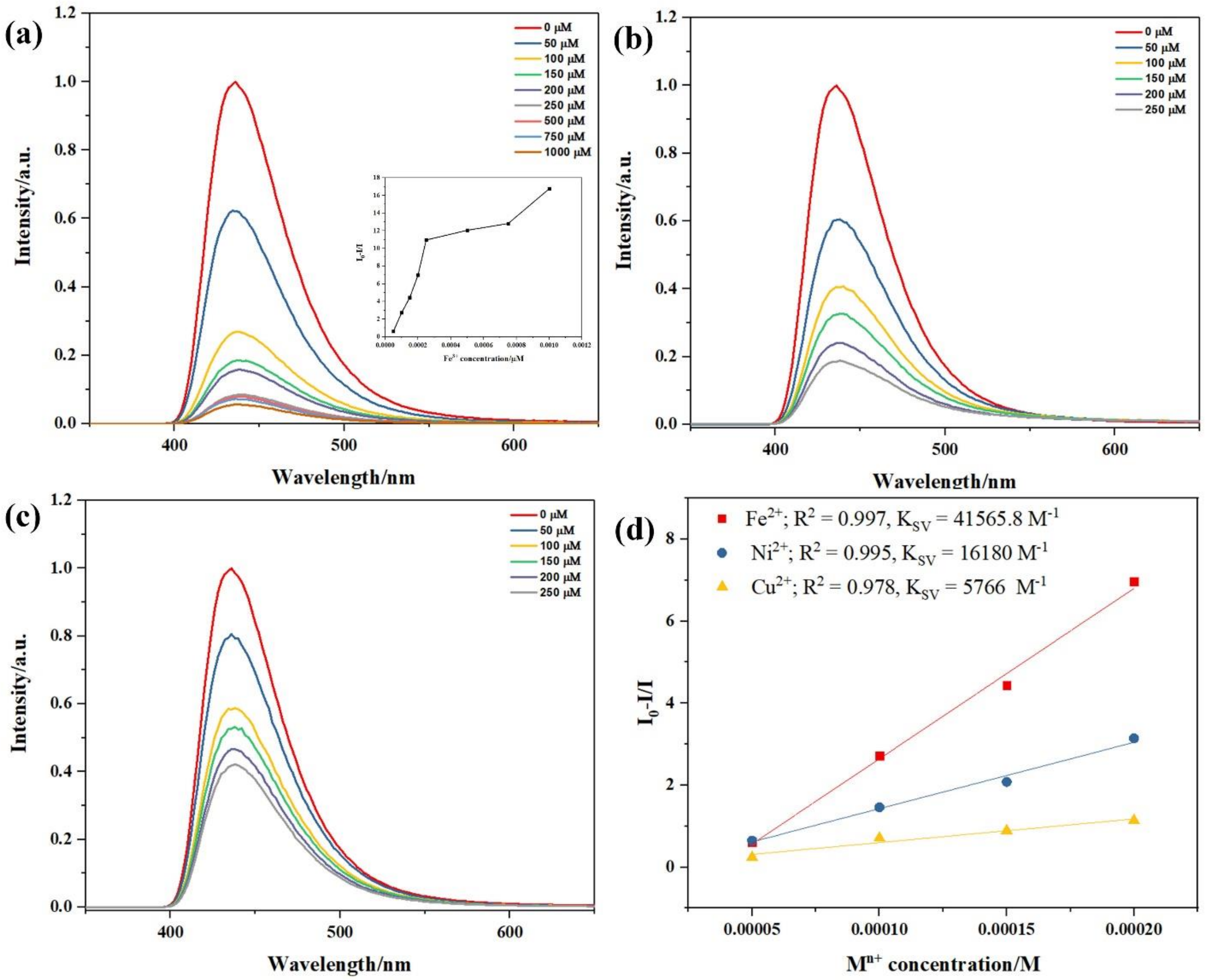

Figure 5. The luminescence spectra of TMU-17-NH_2 with different concentration of (a) Fe^{3+}, (b) Ni^{2+} and (c) Cu^{2+} ions. Inset of (a): Stern-Völmer (SV) plots of the fluorescence emissions of TMU-17-NH_2 quenched by Fe^{3+} in DMF with 270 nm excitation (emission decays were monitored at 440 nm). (d) SV plots of the fluorescence emissions of TMU-17-NH_2 quenched by different metal ions in DMF with 270 nm excitation (λ_{em} = 440 nm).

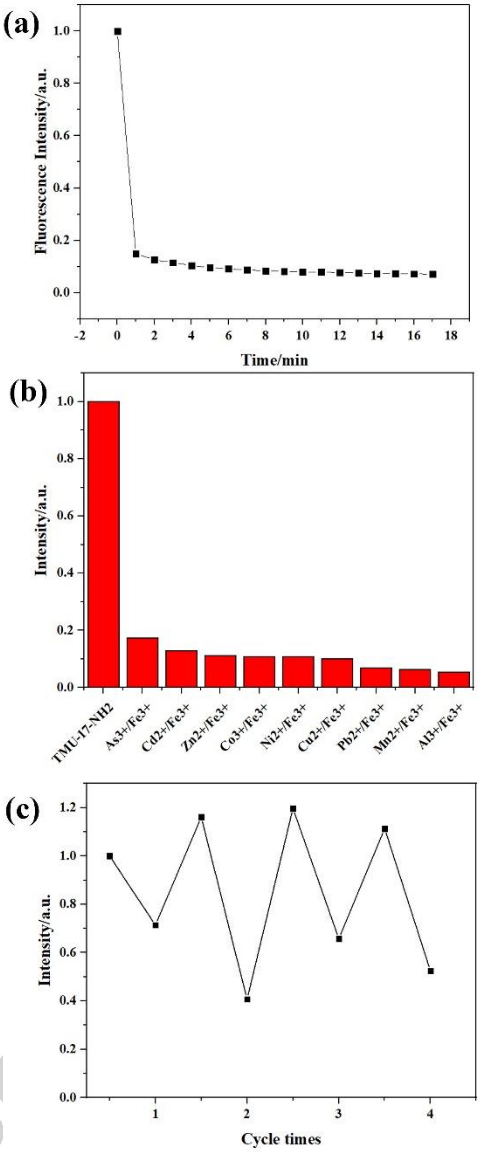

Figure 6. (a) Fluorescence quenching of TMU-17-NH$_2$ by 250 μM Fe^{3+} in DMF as a function of time (λ_{ex}= 270 nm). (b) Comparison of the luminescence intensity of TMU-17-NH$_2$ with 150 μM Fe^{3+} in DMF in presence of 250 μM of other metal ions, monitored at 270 nm. (c) Quenching and recovery tests of TMU-17-NH$_2$ for 100 μM Fe^{3+} in DMF.

Table 1. TMU-17-NH_2 sensing parameter comparison with other MOF based Fe^{3+} sensors.

MOF	**K_{SV} (M^{-1})**	**Detection limit (μM)**	**Line range**	**Ref**
Eu^{3+}@MIL-53-COOH (Al)	5.12×10^3	0.5	0-0.5 mM	[27]
BUT-15	1.66×10^4	0.8	20-700 μM	[46]
BUT-14	2.17×10^3	3.8	20-700 μM	[46]
$[Cd(L)(BPDC)]\cdot 2H_2O$	3.63×10^4	2.21	0.0025-0.15 mM	[47]
$[Cd(L)(SDBA)(H_2O)]\cdot 0.5H_2O$	3.59×10^4	7.14	0.0025-0.15 mM	[47]
$[Cd(ATA)(L)]\cdot 2H_2O$	3.838×10^3	1.77	0-2 mM	[48]
$[Zn(ATA)(L)]\cdot H_2O$	0.557×10^3	3.76	0-2 mM	[48]
$[Eu(HL)(DMF)(H_2O)_2]\cdot 3H_2O$	1.519×10^3	–	0-5 mM	[49]
$[Tb(HL)(DMF)(H_2O)_2]\cdot 3H_2O$	4.479×10^3	50	0-5 mM	[49]
$[Eu(L)(BPDC)_{1/2}(NO_3)]\cdot H_3O$	5.16×10^4	0.5	-	[50]
$[Tb(L)(BPDC)_{1/2}(NO_3)]\cdot H_3O$	4.30×10^4	0.5	-	[50]
[Cd(5-asba)(bimb)]	1.78×10^4	0.0061	0.01875-0.225 mM	[51]
$[Eu_2K_2(dcppa)_2(H_2O)_6].5H_2O$	4.3×10^4	1	10^{-6}-10^{-2} M	[52]
TMU-17-NH_2	4.2×10^4	0.7	50-250 μM	This works